Climate network structure evolves with North Atlantic Oscillation phases

2012 EPL 98 38006

(http://iopscience.iop.org/0295-5075/98/3/38006)

A Letters Journal Exploring the Frontiers of Physics

May 2012

EPL, **98** (2012) 38006
doi: 10.1209/0295-5075/98/38006

www.epljournal.org

Climate network structure evolves with North Atlantic Oscillation phases

O. Guez[1(a)], A. Gozolchiani[1], Y. Berezin[1], S. Brenner[2] and S. Havlin[1]

[1] *Minerva Center and Department of Physics, Bar-Ilan University - Ramat-Gan 52900, Israel*
[2] *Department of Geography, Bar-Ilan University - Ramat-Gan 52900, Israel*

received 18 January 2012; accepted in final form 3 April 2012
published online 11 May 2012

PACS 89.75.-k – Complex systems
PACS 93.30.Mj – Atlantic Ocean
PACS 05.40.-a – Fluctuation phenomena, random processes, noise, and Brownian motion

Abstract – We construct a network from climate records of temperature and geopotential-height in two pressure levels at different geographical sites in the North Atlantic. A link between two sites represents the cross-correlations between the records of each site. We find that within the different phases of the North Atlantic Oscillation (NAO) the correlation values of the links in the climate network are significantly different. By setting an optimized threshold on the correlation values, we find that the number of strong links in the network increases during times of positive NAO indices, and decreases during times of negative NAO indices. We find a pronounced sensitivity of the network structure to the NAO oscillations which is significantly higher compared to the observed response of spatial average of the climate records. Our results suggest a new measure that tracks the NAO pattern.

Introduction. – A network approach has recently been applied in order to follow climate dynamics [1,2]. The nodes of the climate network are geographical sites. The dynamics recorded in each site is composed of its intrinsic dynamics and the coupling with the dynamics of other sites. The cross-correlations due to the coupling between the dynamics in two different sites are represented in our network by a link between the sites (see [3] for a lab experiment that demonstrates the relation between the coupling and the correlation). The maximum value of the correlation might appear with a time delay between the two data records. The climate network approach has recently led to the discovery of several novel insights related to El-Nino dynamics [4–12].

The North Atlantic Oscillation (NAO) is a dominant mode of winter climate variability on a decadal time scale in the North Atlantic region ranging from Central North America to Europe and into Northern Asia. The NAO is a large-scale seesaw in atmospheric mass between the subtropical high and the polar low [13]. The corresponding index is measured by the difference between the mean winter sea level pressure over Azores and over Iceland [14]. It varies from year to year, although it exhibits a tendency to remain in one phase for intervals lasting several years [15].

In this paper we concentrate on the collective behavior of the nodes and links of the climate network during the different NAO phases. In the next section we describe the methods we used, including the data and the numerical procedure. In the results section we present our results, including also a comparison with a method that does not involve the second moment (correlations) and implications. In the last section we summarize and discuss the possible implications of our findings.

Methods. –

Data. We analyze the National Center for Environmental Prediction/National Center for Atmospheric Research (NCEP/NCAR) reanalysis air temperature field at 500 hPa (data set (a)) and 1000 hPa (data set (c)), and geopotential-height field at 500 hPa (data set (b)) and 1000 hPa (data set (d)) [16]. For each node of the network, daily values for the period 1948–2010 are used, from which we extract anomaly values (actual values minus the climatological averaged over the years for each day).

The data is arranged on a grid latitude-longitude with a resolution of $2.5° \times 2.5°$. The location on the globe of the studied region is shown in fig. 1 where the NAO is

(a) E-mail: odedjh@hmail.ph.biu.ac.il

$$C^{y}_{m,n}(\tau>0)\equiv\frac{|\langle[D^{y}_{m}(d)-\langle D^{y}_{m}(d)\rangle]\cdot[D^{y}_{n}(d+\tau)-\langle D^{y}_{n}(d+\tau)\rangle]\rangle|}{\sqrt{\langle[D^{y}_{m}(d)-\langle D^{y}_{m}(d)\rangle]^{2}\rangle}\cdot\sqrt{\langle[D^{y}_{n}(d+\tau)-\langle D^{y}_{n}(d+\tau)\rangle]^{2}\rangle}}, \tag{1}$$

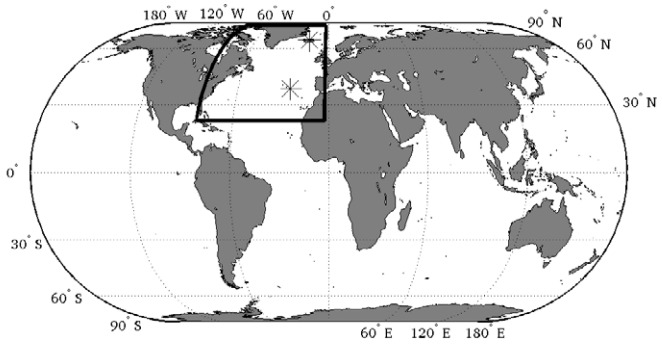

Fig. 1: The geographical region analyzed is [(22.5°–82.5°)N, (2.5°–82.5°)W]. The Azores station is Ponta Delgada (37.7°N, 25.7°W), shown as the lower star. The Iceland station is Akureyri (65.7°N, 18.1°W), shown as the upper star [17].

known to affect [17], and includes the Icelandic-Low and the Azores-High pressure centers, where the NAO index is measured [18]. In this zone there are 33 grid nodes in the East-West direction and 25 grid nodes in the North-South direction, amounting to total of 825 grid nodes (sites). Thus, the total number of links (pairs of sites) is 339000.

Numerical procedure. We first quantify the correlation value of the links, which characterizes the interdependence of the different pairs of sites. We compute for each pair of sites the Pearson correlation function (see, *e.g.*, [19]):

see eq. (1) *above*

$$C^{y}_{m,n}(\tau<0)\equiv C^{y}_{m,n}(\tau>0), \tag{2}$$

where m and n are the indices of the two sites. D is the data record and d is the day index, ranging between 1 and 122 (1st December of the current year to 1st April of the following year). We chose to analyze only the Winter season when the NAO effects are known to be stronger (see, *e.g.*, [14]). The parameter τ is the time lag, ranging between -72 and $+72$ days y is the year, ranging between 1948 and 2010.

The Pearson correlations, $C^{y}_{m,n}$, are computed from data that begins in the year represented by y and ends in $y+2$. This choice is made in order to have sufficient statistics as well as to capture the dynamical changes of these correlations. Upper limits of $y, y+1, y+3, y+4$ yield similar results but less pronounced (not shown).

To better quantify the interdependence of the different pairs of sites we define the strength of the link as the highest correlation value with respect to the background noise (see [2]). Thus, the strength of the link in year y, connecting the sites m and n, $S^{y}_{m,n}$, is defined as follows:

$$S^{y}_{m,n}=\frac{MAX\left(C^{y}_{m,n}\right)-MEAN\left(C^{y}_{m,n}\right)}{STD\left(C^{y}_{m,n}\right)}. \tag{3}$$

The average ($MEAN$) and standard deviation (STD) are taken over all τ values, $-72\leqslant\tau\leqslant+72$.

To test whether and how the dynamics of these links is related to NAO, we build a network composed of links stronger than a given threshold value H. The existence (1) or nonexistence (0) of a strong link is represented in the time-dependent adjacency matrix of the network:

$$B^{y}_{m,n}(H)=S^{y}_{m,n}\cdot\Theta\left(S^{y}_{m,n}-H\right), \tag{4}$$

where $\Theta(x)$ is the unit step function (Heaviside).

Summing $B^{y}_{m,n}(H)$ overall pairs m, n for a given year y yields the time series of the number of the links in the network, for a given H:

$$\sigma_{H}(y)=\sum_{m>n}B^{y}_{m,n}(H). \tag{5}$$

Results. – Here we explore a relation between the structure of the climate network and the NAO events.

The influence of the NAO on the number of links in the network. We calculate the number of links in each year y, $\sigma_H(y)$, that are stronger than a threshold H. Then we compute the correlation $R(H)$ between $\sigma_H(y)$ and the NAO index, $I(y)$. To estimate the error in $R(H)$ we randomly divide the 339000 pairs into 20 sub-networks. We perform the analysis described above for each sub-network. The standard deviation of $R(H)$ of the twenty sub-networks is the estimator of the error. We systematically compute the correlation $R(H)$ for different H values shown as the black curve in fig. 2. The same is also preformed with a surrogate data (explained later in the section of validation tests) shown as the gray curve in fig. 2.

For example, for data set (d) one can see that for $H<5.2$ the correlation $R(H)$ of the real data is comparable to the correlation $R(H)$ of the surrogate data. However, for higher values of H there is a broad range of thresholds for which the correlation $R(H)$ of the real data is significantly higher than the correlation $R(H)$ of the surrogate data. We define the optimal threshold, H^*, as the one which yields the maximal correlation, $R(H^*)$. The values of $R(H^*)$ for all data sets are given in table 1. For data set (d) the value $H^*=6.1$ is the optimal threshold, at which $R(H^*)=0.50\pm0.01$ is the maximal correlation. Similar behavior is seen for the other data sets.

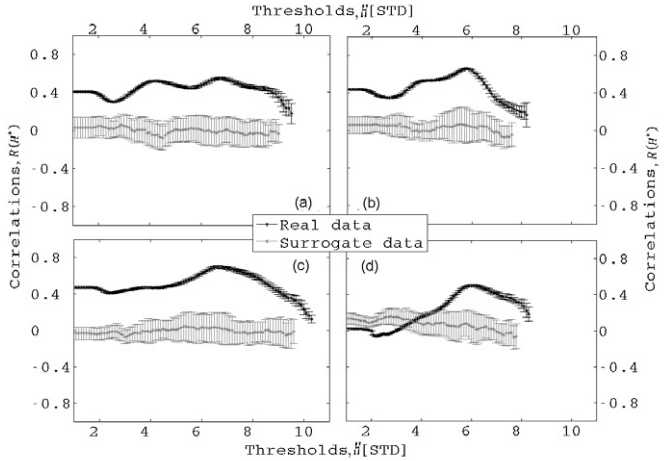

Fig. 2: The correlation, $R(H)$, between the number of the strong links, $\sigma_H(y)$, and the NAO index, $I(y)$, as a function of the threshold, H, for the real data (black) and the surrogate data (gray). The four panels describe the behavior of the network of four data sets: (a) air temperature field at 500 hPa; (b) geopotential-height field at 500 hPa; (c) air temperature field at 1000 hPa; (d) geopotential-height field at 1000 hPa.

Table 1: The values of the correlations for different methods.

Data Set	$R(H^*)$	$\tilde{R}$
(a)	$+0.55 \pm 0.01$	-0.16 ± 0.09
(b)	$+0.66 \pm 0.01$	-0.39 ± 0.09
(c)	$+0.70 \pm 0.01$	-0.28 ± 0.12
(d)	$+0.50 \pm 0.01$	-0.26 ± 0.01

The values of the correlations $R(H^*)$ between the number of the strong links, $\sigma_{H^*}(y)$, and the NAO index, $I(y)$, at the optimal threshold, H^*. The values of the correlations $\tilde{R}$ between the average of all the records, $\Delta(y)$, and the NAO index, $I(y)$. The four lines show the correlations for four types of data sets: (a) air temperature field at 500 hPa; (b) geopotential-height field at 500 hPa; (c) air temperature field at 1000 hPa; (d) geopotential-height field at 1000 hPa.

Implications. We show in fig. 3 the behavior of the number of the strong links, $\sigma_{H^*}(y)$, in comparison with the NAO index, $I(y)$.

In fig. 3, one can see that $\sigma_{H^*}(y)$ obtains high values when $I(y)$ is positive and vice versa. This behavior suggests a positive correlation between the number of links in the network and the NAO index (see also $R(H^*)$ in table 1). However, the Average Field Test (described next), $\Delta(y)$, obtains high values when $I(y)$ is negative and vice versa. This behavior suggests a surprisingly negative (not negligible) correlation between the average of all the records and the NAO index (see also $\tilde{R}$ in table 1).

Average Field Test. In the previous section we estimated the sensitivity of the links of the climate network to the NAO. Next we wish to estimate the sensitivity of the average records of the sites themselves to the NAO. For this we calculate the average of all the records shown

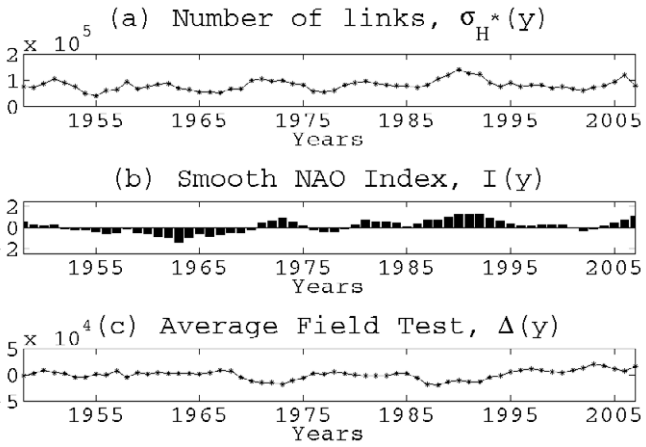

Fig. 3: (a) The number of the strong links, $\sigma_{H^*}(y)$, for the optimal threshold, $H^* = 6.8$, for data set (c), air temperature field at 1000 hPa. (b) The smooth NAO index, $I(y)$. (c) The Average Field Test, $\Delta(y)$, for data set (c), geopotential-height field at 500 hPa.

in fig. 1:

$$\Delta(y) \equiv \langle\langle D_m^y(d)\rangle_d\rangle_m , \tag{6}$$

where m is the index of the site. $D_m^y(d)$ is the data record and d is the day index, ranging between 1 and 122 (1st December of the current year to 1st April of the following year). The symbol $\langle\ \rangle_d$ represents averaging over the Winter days and the symbol $\langle\ \rangle_m$ represents averaging over all sites. The error of the values of the correlation is estimated using the standard deviation of sub-networks mentioned earlier.

Next, we calculate the correlation $\tilde{R}$ between the NAO index, $I(y)$, and the average of all the records, $\Delta(y)$. The comparison between the correlations $R(H^*)$ and $\tilde{R}$ are shown in table 1.

One can see that for all data sets the absolute value of $\tilde{R}$ is significantly smaller than the value of $R(H^*)$. This indicates that the sensitivity of the number of strong links in the network to the NAO is higher compared with the sensitivity of the average of all the records.

Validation tests. Here we present two validation tests for the significance of our results for the correlations of the real data with the NAO index, $R(H)$.

The first validation test is performed by using surrogate data sets series to build in climate networks. This is obtained by shuffling full years in the time records of each site, keeping the order within each year unchanged. The correlation $R(H)$ of the network built by the surrogate data series is shown in fig. 2. Previous work [20] has shown that cross-correlations are influenced by the auto-correlations of the signals [21]. Higher auto-correlations within the signals yield stronger cross-correlations, even when there is no coupling between the two signals. In this validation test we conserve the natural auto-correlation in each sequence and fig. 2 indicates that what we find is mostly due to pure cross-correlations.

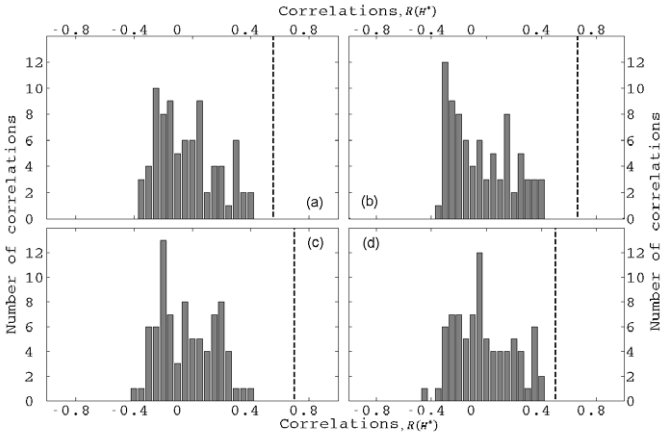

Fig. 4: The histograms (gray bar) of the correlation values between the number of the strong links, $\sigma_{H^*}(y)$, and the surrogate indices, $I_Y(y)$, and the correlation values $R(H^*)$ (black line, given in fig. 1). The four panels describe the behavior of the network of four types of data sets: (a) air temperature field at 500 hPa; (b) geopotential-height field at 500 hPa; (c) air temperature field at 1000 hPa; (d) geopotential-height field at 1000 hPa.

The second validation test is performed by comparing the correlation $R(H^*)$ to correlation with sequences that have the same dynamical behavior as the NAO index, but not in the same years. For this purpose we use earlier data of NAO index in the years 1823–2001 [22] to compute the extended NAO indices:

$$I_Y(y); \quad Y = 1865, \ldots, 1945, \tag{7}$$

where the sub-index Y is the first year of the surrogate sequence. This way we form 81 surrogate sequences (configurations) each with the same length (59 years) like the NAO index, $I(y)$. Each sequence is shifted by 1 year.

We calculate the correlations between the number of the strong links, $\sigma_{H^*}(y)$, and each one of the surrogate sequences, $I_Y(y)$. We show in fig. 4 the histogram of the correlation values, for each of the 4 data sets mentioned above.

One can see that for all data sets the real correlation (mark with a dashed line) is significantly higher than all of the surrogate correlation values.

Summary. – We find that the NAO variations influence the number of strong links (high correlations) in the climate network. In particular, for negative index periods we observe the weakening of many strong links, which appear during positive index periods. We also find that there is a broad range of correlation values that is most sensitive to the NAO. Our results suggest that the links in the climate network are more sensitive to NAO variations compared to the temperature or pressure changes.

* * *

We wish to thank Prof. K. Yamasaki for useful discussions.

REFERENCES

[1] Tsonis A. A., Swanson K. L. and Roebber P. J., *Am. Meteorol. Soc.*, **87** (2006) 585.
[2] Yamasaki K., Gozolchiani A. and Havlin S., *Phys. Rev. Lett.*, **100** (2008) 228501.
[3] Castrejo'n-Pita A. A. and Read P. L., *Phys. Rev. Lett.*, **104** (2010) 204501.
[4] Gozolchiani A., Yamasaki K., Gazit O. and Havlin S., *EPL*, **83** (2008) 28005.
[5] Tsonis A. A., Swanson K. L. and Wang G., *J. Clim.*, **21** (2008) 2990.
[6] Tsonis A. A. and Swanson K. L., *Phys. Rev. Lett.*, **100** (2008) 228502.
[7] Tsonis A. A., *Int. J. Bifurcat. Chaos*, **17** (2007) 4229.
[8] Gozolchiani A., Yamasaki K. and Havlin S., *Phys. Rev. Lett.*, **107** (2011) 148501.
[9] Donges J. F., Schultz H. C. H., Marwan N., Zou Y. and Kurths J., *Eur. Phys. J. B*, **84** (2011) 4 635.
[10] Donges J. F., Zou Y., Marwan N. and Kurths J., *Eur. Phys. J. ST*, **174** (2009) 157.
[11] Donges J. F., Zou Y., Marwan N. and Kurths J., *EPL*, **87** (2009) 48007.
[12] Wang G., Swanson K. L. and Tsonis A. A., *Geophys. Res. Lett.*, **36** (2009) L07708.
[13] Van Loon H. and Rogers J., *Mon. Weather Rev.*, **106** (1978) 296.
[14] Walker G. T. and Bliss E. W., *World Weather V. Mem. R. Meteorol. Soc. 4*, **36** (1932) 53.
[15] `www.ldeo.columbia.edu/res/pi/NAO/`.
[16] Kalnay E., Kanamitsu M., Kistler R., Collins W., Deaven D., Gandin L., Iredell M., Saha S., White G., Woollen J., Zhu Y., Leetmaa A. and Reynolds R., *Bull. Am. Meteorol. Soc.*, **77** (1996) 437.
[17] Feldstein S. B., *Q. J. R. Meteorol. Soc.*, **129** (2003) 901.
[18] Jones P. D., Jonsson T. and Wheeler D., *Int. J. Climatol.*, **17** (1997) 1433.
[19] Press W. H., Teukolsky S. A., Vetterling W. T. and Flannery B. P., *Numerical Recipes in C* (Cambridge University Press) 1992.
[20] Podobnik B., Fu D. F., Stanley H. E. and Ivanov P. Ch., *Eur. Phys. J. B*, **56** (2007) 47.
[21] Koscielny-Bunde E., Bunde A., Havlin S., Roman H. E., Goldreich Y. and Schellnhuber H. J., *Phys. Rev. Lett.*, **81** (1998) 729.
[22] `http://www.cru.uea.ac.uk/cru/data/nao.html`.